Inorganica Chimica Acta xxx (2016) xxx–xxx

Contents lists available at ScienceDirect

Inorganica Chimica Acta

journal homepage: www.elsevier.com/locate/ica

The phosphate clamp as recognition motif in platinum–DNA interactions

Seiji Komeda [a,b], Yun Qu [a], John B. Mangrum [a], A. Hegmans [a], Loren D. Williams [b], Nicholas P. Farrell [a,*]

[a] Department of Chemistry, Virginia Commonwealth University, 1001 W. Main Street, Richmond, VA 23284-2006, United States
[b] School of Chemistry and Biochemistry, Georgia Institute of Technology, Atlanta, GA 30332-0400, United States

ARTICLE INFO

Article history:
Received 27 January 2016
Received in revised form 24 April 2016
Accepted 30 April 2016
Available online xxxx

Keywords:
Platinum–DNA
Phosphate clamp
Polyamines

ABSTRACT

This review summarizes studies on substitution-inert polynuclear platinum complexes (PPCs) which bind to DNA through the phosphate clamp – a discrete mode of DNA–ligand recognition distinct from the canonical intercalation and minor-groove binding. Especially, this review concentrates on comparing the binding and conformational changes induced by trinuclear platinum complexes with dinuclear spermine-linked complexes. The protonated central polyamine $-^{+}NH_2-(CH_2)_4-N^{+}H_2-$ of spermine allows direct comparison with the central Pt(tetraamine) moiety of the trinuclear complexes. The weight of the evidence suggests that while overall charge on the small molecule determines binding affinity, the presence of minor groove spanning from the phosphate clamp is important in conformational changes and in sequence selectivity.

1. Introduction

In coordination and organometallic chemistry, reactions on DNA and RNA nucleic acid templates are broadly divided into covalent bond-forming reactions and "non-covalent" association or molecular recognition through a combination of electrostatic, π–π stacking and hydrogen-bonding interactions. In the case of platinum, the understanding of cisplatin ([*cis*-$PtCl_2(NH_3)_2$, *cis*-DDP] antitumor activity has to some extent dominated Pt–DNA studies, where that activity is predicated on the need for formation of Pt–DNA bonds. The associative nature of substitution reactions on square planar platinum automatically allows for systematic study of structural effects (such as hydrogen-bonding) and steric effects in dictating rates of reaction, base specificity and conformational changes on cisplatin–DNA adducts. Pre-association of the small molecule on the polymer template may also affect the final profile of the covalent Pt–DNA adducts.

The pre-association on DNA of small molecules such as cisplatin may be studied using fast spectroscopic techniques but also by using substitution-inert analogs. For example the association of the relatively simple $[Pt(NH_3)_4]^{2+}$ cation on nucleotides has been studied by NMR relaxation methods using the ^{15}N-labeled sample [1]. IR and ^{1}H NMR studies confirmed the persistence in solution for the $[Pt(en)_2]^{2+}$-5′-GMP cation–anion pair through H-bonding [2]. Outer-sphere association constants for $[Pt(NH_3)_4]^{2+}$ and $[Pt(pyr)_4]^{2+}$ on 20-mer oligonucleotides have been determined by ESI Mass Spectrometry [3]. In this example, association constants for both single-stranded and double-stranded DNA could be calculated. Association constants for dsDNA were approximately twice as large as for the corresponding individual ssDNA. Cumulative association constants were also calculated for binding of more than one Pt unit. Fewer association sites were available for the more sterically demanding $[Pt(pyr)_4]^{2+}$ cation [3].

1.1. Polynuclear platinum complexes

It is axiomatic that as the positive charge increases on the small molecule the residence time on the negatively-charged oligonucleotide should be higher. In this respect, highly-charged substitution-inert polynuclear platinum complexes (PPCs) with [Pt(tetraam(m)ine] coordination spheres have given much information and novel insights into conformational changes on the polynucleotide. PPCs in general represent a discrete class of antitumor agents with wide capacity for diversity given their general structure (Fig. 1). A specific example is Triplatin (BBR3464) which underwent Phase II human clinical trials, and whose clinical results have been reviewed [4–6]. Triplatin–DNA interactions are distinct from the mononuclear cisplatin and oxaliplatin and, indeed, unlike those of any agent in clinical use.

PPC–DNA adducts (and their subsequent biological consequences) are structurally distinct from those formed by the

Abbreviations: en, ethylenediamine; 5′-GMP, 5′-guanosine monophosphate; pyr, pyridine.

* Corresponding author. Tel.: +1 804 828 6320; fax: +1 804 828 8599.
E-mail address: npfarrell@vcu.edu (N.P. Farrell).

http://dx.doi.org/10.1016/j.ica.2016.04.052
0020-1693/

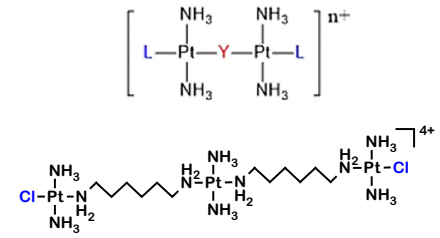

Fig. 1. (Top) general structure of charged polynuclear platinum complexes. Where L = X^-(Cl^-) covalently-binding complexes are formed. Replacement of X^- by L = NH_3 or the dangling amine $-H_2N(CH_2)_nNH_3^+$ affords the substitution-inert series. (Bottom) specific structure of the clinical drug Triplatin (BBR3464).

mononuclear cisplatin and congeners. The PPC–DNA binding profiles have been reviewed in relationship to the antitumor activity of the series [5,6]. The high positive charge of these compounds has allowed for observation of pre-association effects on DNA by NMR and Mass Spectroscopy [7–9]. Notably, the formation of novel directional {Pt,Pt} 5′–5′ and 3′–3′ interstrand crosslinks may be associated with pre-association on the DNA template [10,11]. The role of pre-association in dictating competitive binding preferences between {Pt,Pt} intrastrand and interstrand crosslinks has also been studied [12].

1.2. Substitution-inert polynuclear platinum complexes

The substitution-inert complexes, prepared by substitution of Cl^- with either NH_3 or a "dangling amine" where one end of the diamine is linked to Pt with the other end free and protonated are now recognized as a distinct sub-class within the PPC structure with their own DNA-binding profiles and biological activity (Fig. 2). More recently we have reviewed the DNA binding and cellular biology of these substitution-inert PPCs [4]. The trinuclear structures of Fig. 2 show a superficial resemblance to the free biologically important polyamines spermidine and spermine. Incorporation of the linear polyamines into the basic polynuclear framework of Fig. 1 (Y = spermidine or spermine, L = Cl) by replacement of the central tetraa(m)mine unit of Triplatin produces a series of dinuclear compounds which replicate the biological activity of the trinuclear drug [13,14]. The DNA binding profiles, including the rate of association and especially the preferred formation of long-range {Pt,Pt} inter-strand crosslinks, have been compared to the dinuclear and trinuclear complexes bridged by the simple 1,6-hexanediamine [15].

A reasonable question is how the substitution-inert PPCs differ in their DNA binding properties to the free polyamines. Earlier studies showed that dinuclear compounds $[\{Pt(NH_3)_3\}_2\mu\text{-}(H_2N(CH_2)_nNH_2)]^{4+}$ were effective initiators of the B → Z and B → A conformational transitions in suitable DNA sequences and significantly more effective than spermine itself [16,17]. In this review article we summarize the DNA-binding properties of the three compounds of Fig. 2 and contrast them with the related DNA-binding polyamines themselves as well as the canonical minor groove binders such as Hoechst Dye 33258.

2. Solid state structures

Extension to trinuclear substitution-inert compounds was originally envisaged to examine the pre-association phenomenon on biomolecules and its role in the pharmacokinetics of Triplatin, in the absence of Pt–DNA bond formation. The X-ray crystal structure determination of the adduct between TriplatinNC (**III**) and the Dickerson–Drew Dodecamer (DDD, $[d(CGCGAATTCGCG)]_2$) added further relevance and a significant new direction through recognition of a discrete new manner of DNA binding – the phosphate clamp, a new mode of ligand–DNA recognition distinct from the conventional modes of intercalation and groove binding (NDB entry 2DYW) [18]. Hydrogen bonding with phosphate oxygens results in either backbone tracking or groove spanning through formation of "phosphate clamps" where the square-planar tetra-am(m)ine Pt(II) coordination units all form bidentate N–O–N complexes with phosphate oxygen OP atoms, Scheme 1. The generality of the motif was confirmed by a second crystal and molecular structure with TriplatinNC-A (**II**) – that is with L = NH_3 (6+) instead of $-NH_2(CH_2)_6NH_3^+$ (8+) [19]. The geometry of the phosphate clamp is remarkably conserved in both structures. In both cases, the conformation in the DDD-phosphate clamp complexes differs significantly from that of the native structure (NDB entry BDL084) [18,19].

Within the substitution-inert class, systematic changes allow synthesis of dinuclear complexes such as $[\{Pt(NH_3)_3\}_2\text{-}\mu\text{-spermidine}]^{5+}$ and $[\{Pt(NH_3)_3\}_2\text{-}\mu\text{-spermine}]^{6+}$ connected *via* polyamine central linkers rather than the central {Pt(tetraamine)} unit of the trinuclear compounds [20,21]. The protonated central polyamine $-^+NH_2-(CH_2)_4-N^+H_2-$ of spermine allows direct comparison

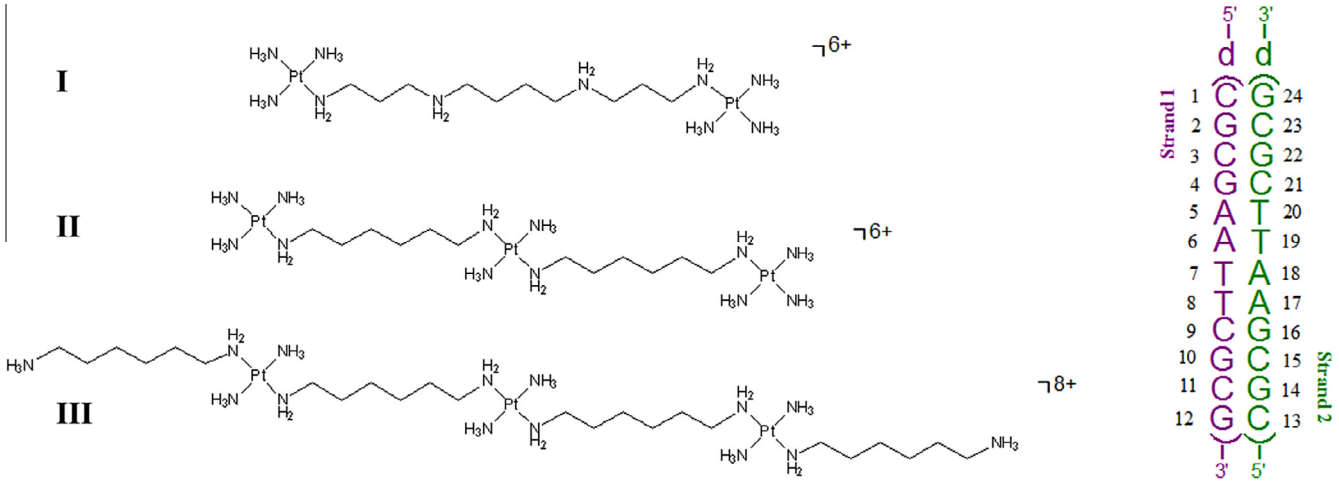

Fig. 2. Structures of substitution-inert polynuclear platinum complexes and the 12-mer Dickerson–Drew duplex (DDD) used for crystallography studies. **I** is abbreviated DiplatinNC–spm, **II** is TriplatinNC-A and **III** is TriplatinNC.

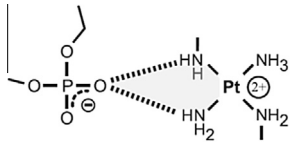

Scheme 1. The molecular description of the phosphate clamp.

with the central Pt(tetraamine) moiety of the trinuclear complexes and strict comparison of the effects of the phosphate clamp *versus* the polyamine motif since the molecules **I** and **II** of Fig. 2 have identical charge (6+).

2.1. Solid state structure of a spermine-linked dinuclear platinum complex

In this section we compare the solid-state structures of the DDD adducted to the compounds of Fig. 2. Also compared is the structure of TriplatinNC–DDD (TriplatinNC/spm) but crystallized in the presence of spermine, which is commonly used in DNA crystallizations. The emphasis will be on the spermine-linked compound. The crystallographic data are summarized in Table 1. Diffraction data from the DDD—DiplatinNC–spm and DDD—TriplatinNC/spm structures extend to 1.42 and 1.40 Å, respectively. For the former structure the final refined model of the asymmetric unit of a crystal contain (i) a DDD, (ii) a partially disordered DiplatinNC–spm molecule, (iii) four bare platinum(II) ions (substantially disordered DiplatinNC–spm) with low occupancies and (iv) a hexa-hydrated Mg^{2+} ion, and (v) 93 water molecules. The hydrogen-bonding interactions are shown in Fig. 3. For the latter TriplatinNC/spm structure the asymmetric unit contains (i) a DDD, (ii) a TriplatinNC molecule, (iii) one bare platinum(II) ion (substantially disordered TriplatinNC molecule) and (iv) 100 water molecules, and no clear Mg–H_2O or Na–H_2O water coordination spheres were observed. The hydrogen-bonding interactions are similar to that previously seen for the structure in absence of spermine, [18], and are shown in Fig. S1. The occupancy ratio of DDD—TriplatinNC/spm crystallized in the presence of spermine was found to be significantly lower than that of DDD—TriplatinNC, crystallized in the absence of spermine, probably due to some competitive association with spermine.

A comparison of potential backbone tracking shows a phosphate clamp at C13 for the spermine-linked compound (Fig. 4). Notably, it appears that this is formed from mutually *cis* NH_3 ligands of a *cis*-{$Pt(NH_3)_2$} unit rather than the *cis*-{$Pt(NH_3)(NH_2$-CH_2–)} of the trinuclear compounds. The presence of the central polyamine –$^+NH_2$– units allows H-bonding from the spermine ligand to the phosphate backbone. The absence of a suitably placed second Pt coordination sphere affects the overall structure. The backbone tracking of the three compounds are compared in Fig. 5. In this case the two Pt coordination spheres are not the right distance apart to form the groove spanning motif and instead only weak H-bonds from both the Pt coordination sphere and the central spermine are observed. Both the comparisons of backbone tracking and groove spanning show the importance of optimally positioned Pt coordination spheres to achieve the maximal effects. The major structural parameters of the DDD affected by the phosphate clamp are helix bending and the impact on the minor and major groove widths. The bending seems to correlate well with the occupancy ratio of Pt(II) to the DDD. The spermine-linked dinuclear compound thus does not seem to affect the bending significantly. The diminished bending observed in the TriplatinNC/spm structure also correlates with the reduced occupancy caused by competition with spermine as noted above. The minor-groove width is not compacted to any significant degree whereas in the case of the major groove more variability is seen, Fig. 6.

3. Gas phase studies

The gas phase stability of duplex DNA–drug complexes has been studied for intercalators and minor groove binders [22,23]. Mass spectrometry has also been used to examine ammonium– or guanidinium–aromatic interactions through cation–π interactions and ammonium– or guanidinium–phosphate interactions through salt bridge formation [23]. Mass Spectrometry has been very useful in studying salt bridge interactions on the gas-phase stability of DNA–peptide complexes [24]. Studies on the phosphate–arginine(guanidinium)/quaternary ammonium salt interactions indicate a remarkably high gas-phase stability [25–27]. Guanidinium-based drug binding to single-stranded DNA has also been extensively studied [28,29].

Table 1
Crystallographic parameters for substitution-inert polynuclear platinum complexes bound to duplex DNA.[a,b]

	TriplatinNC[c]	TriplatinNC-A[d]	DiplatinNC–spm[e]	TriplatinNC/spm[f]
Total No. of Pt(II) ions including Pt complex	4	3	5	4
Number of fully assigned Pt(II) coordination planes	3 + 1	3 – 1	2 – 1	3
Occupancy of Pt complex (assigned as complex)	0.75, 0.60	0.79	0.1	0.55
Occupancy ratio of Pt(II) to DDD duplex	1:2.85	1:1.69	1:0.50	1:2.05
Total number of H-bonds between Pt complex and DDD including PC	27	13	4	16
Total number of phosphate clamps	8	3	1	6
Averaged number of phosphate clamps/fully assigned Pt(II) coordination plane	2	1.5	1	2
Maximum number of phosphate clamps/fully assigned Pt(II) coordination plane	3	2	1	3
Minimum number of phosphate clamps/fully assigned Pt(II) coordination plane	2	1	1	1
DNA bending (11.6 degrees without DNA ligand)	26.2	18.0	11.4	22.7
Binding mode	Backbone-tracking Groove-spanning	Backbone-tracking Groove-spanning	Phosphate clamp weak H-bond between phosphate and spermine	Backbone-tracking Groove-spanning

[a] See Fig. 2 for structures. See Refs. [18,19] and Supplementary information (text and Tables S1 and S2) for experimental conditions.
[b] TriplatinNC with spm is TriplatinNC–DDD crystallization in presence of spermine and is abbreviated TriplatinNC/spm.
[c] Na-GuaO(6) coordination [18].
[d] Intermediate conformation between TriplatinNC–DDD and DDD [19].
[e] Occupancy of Pt complex is low, and only half of molecule was assigned. Disordered four Pt ions were assigned as bare, without ligands.
[f] Overall, very similar to structure in absence of spermine [18].

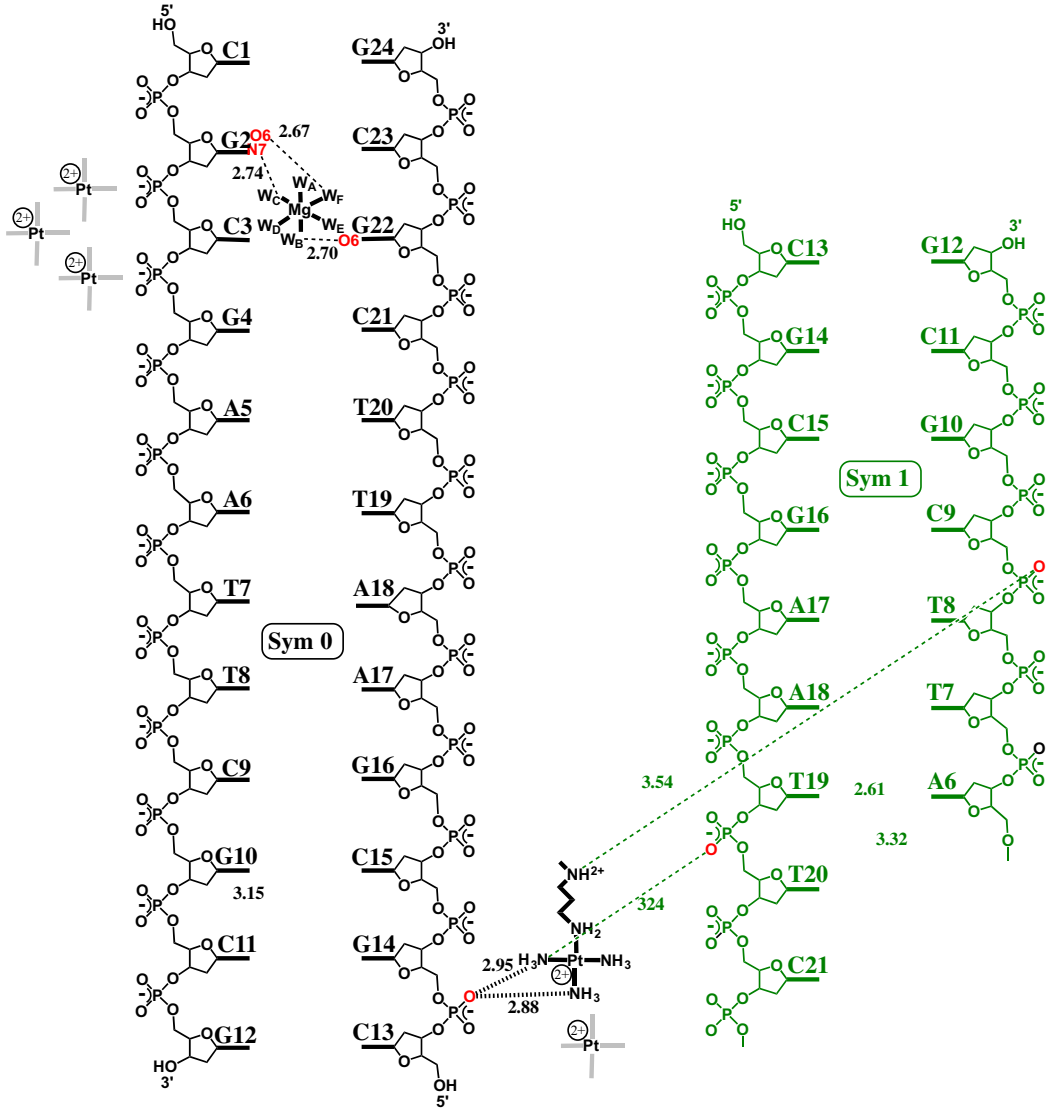

Fig. 3. Hydrogen bonding interactions of DiplatinNC–spm and hexa hydrated Mg^{2+} ion with DNA. Hydrogen bonding interactions of the phosphate clamp is indicated by bold hashed lines. Other hydrogen bonds are indicated by dashed lines. The DNA oxygen and nitrogen atoms that form hydrogen bonds are highlighted in red. Hydrogen bonding distances are given in Angstroms. Intra- and inter-symmetry hydrogen bonding network of DiplatinNC–spm with duplexes. Sym 0: x, y, z; Sym 1: $-x-1, y+1/2, -z+1/2$. (For interpretation of the references to color in this figure legend, the reader is referred to the web version of this article.)

Full scan ESI-MS spectra of dsDNA complexed with substitution-inert polynuclear platinum compounds confirm that the non-bonding interaction is strong enough to be transferred from solution to the gas phase. A 1:1 adduct ratio is characteristically observed because excessive precipitation occurs at higher stoichiometry. The limiting gas-phase dissociation pathways for ligand (drug)–DNA complexes deduced from these studies have been classified as loss of neutral ligand, loss of deprotonated ligand, and ligand remaining bound to a single strand even after separation of the strands, Scheme 2.

The full scan ESI-MS of the free 17-mer duplex AT duplex {5′-TAGCGCTTTTTCCGTA-3′}–{5′-TACGCGAAAAAGCGCTA-3′} and also when adducted to the substitution-inert compounds gave observable series of peaks corresponding to 6-, 7- and 8-charge states. The 7-charge state was chosen for further study as the intensity was highest. The CID (Collision Induced Dissociation) spectra of the $[dsDNA-7H]^{7-}$ (m/z 1481) at three different collisional energies, 10, 16, and 22 eV are shown in Fig. 7. The free dsDNA dissociates readily with the seven available charges distributed into the $[ssDNA-4H]^{4-}$ (at m/z 1290 and 1302) and $[ssDNA-3H]^{3-}$ (at m/z 1721 and 1736), product ions *via* complete unzipping of the duplex. Due to the high charge state chosen for the CID, there is no covalent backbone cleavage observed as the higher charge aids in the coulombic repulsion of the two strands. The noncovalent bond cleavage producing separation into ssDNA strands is favored in high energy CID instruments such as the Q-TOF2 but at the highest energy a small degree of base loss is observed.

All three platinum agents behave similarly in the CID spectra and there is significant stabilization with respect to free uncomplexed duplex. All three gave a characteristic 1:1 stoichiometry and excessive precipitation is clearly visible upon complexing at higher stoichiometry. The CID spectrum of the 17mer {5′-TAGCGCTTTTTCCGTA-3′}–{5′-TACGCGAAAAAGCGCTA-3′}–TriplatinNC (**III**) adduct ($[dsDNA-7H]^{7-}$, m/z 1481) at three different collisional energies, 10, 16, and 22 eV again shows ready dissociation into the $[ssDNA-4H]^{4-}$ and the $[ssDNA-3H]^{3-}$ product ions *via* complete unzipping of the duplex, at (m/z 1290 and 1302) and

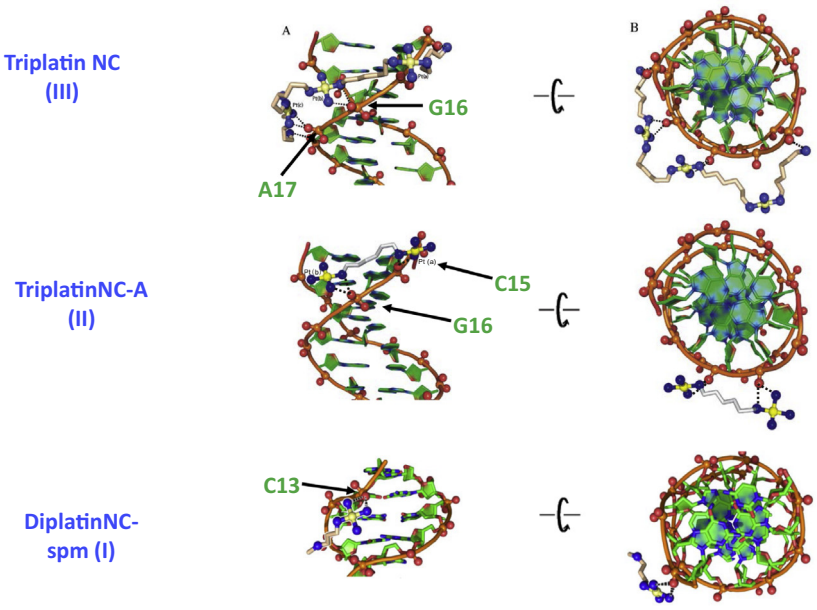

Fig. 4. Comparison of backbone tracking motifs in PPC–DDD structures. See Fig. 2 for structures.

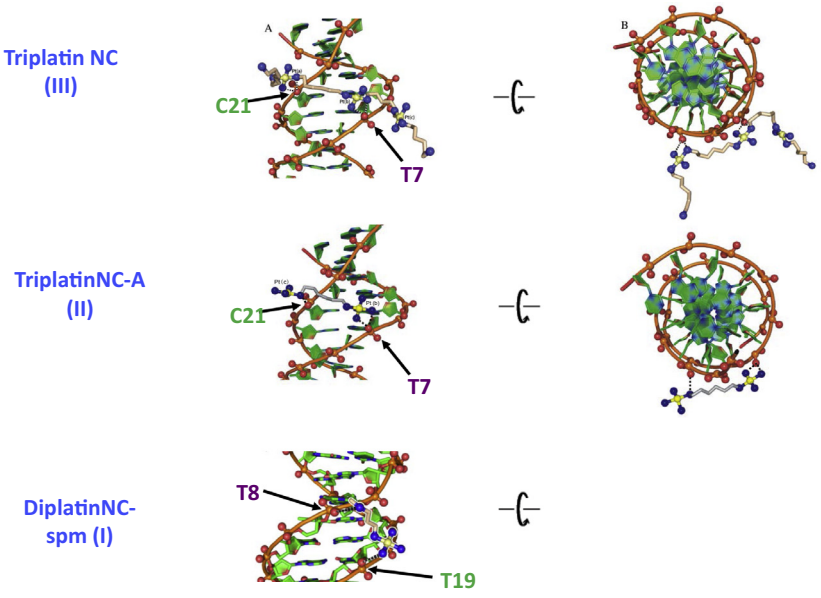

Fig. 5. Comparison of groove spanning in PPC–DDD structures. See Fig. 2 for structures.

(*m*/*z* 1721 and 1736), respectively, Fig. 7. TriplatinNC, **III**, shows the highest degree of dsDNA stabilization, coinciding with the highest charge and number of available hydrogen bonding contacts for phosphate clamp binding motifs. The $CE_{50\%}$ may be defined as approximately the point at which 50% of the duplex remains intact. For TriplatinNC, this extends out to ~30 eV of collisional energy, and strand separation is still the preferred dissociation pathway. Increasing the collisional energy shows that the spermine-linked complex is the least stable of the three dsDNA–Pt complexes. The $[dsDNA+\mathbf{I}-7H]^{-7}$ (*m*/*z* 1581) ion dissociates into $[ssDNA+\mathbf{I}-3H]^{-3}$ (*m*/*z* 1952 and 1968) and the $[ssDNA-4H]^{-4}$, (*m*/*z* 1290 and 1302), Fig. 7. Given the high (7–) charge state chosen for these experiments, minimal covalent backbone fragmentations are observed.

3.1. Comparison with Hoechst Dye 33258

Besides the natural analogies with the polyamines, there is some similarity from solution NMR studies of PPC–DNA studies with the minor groove binding of canonical minor groove binders Hoechst Dye and Netropsin. Specifically, many minor groove contacts are observed in the NMR spectra of substitution-inert PPC–DNA structures, similar to those observed for minor groove binders, Table 2. The CID of Hoechst Dye with duplex DNA conformed to literature reports proceeding with strand separation with the drug remaining bound to either of the two strands, in contrast to the PPCs (Fig. 8).

Fig. 9 compares the gas phase stabilization for each of the noncovalent platinum compounds with the 17-mer dsDNA. The

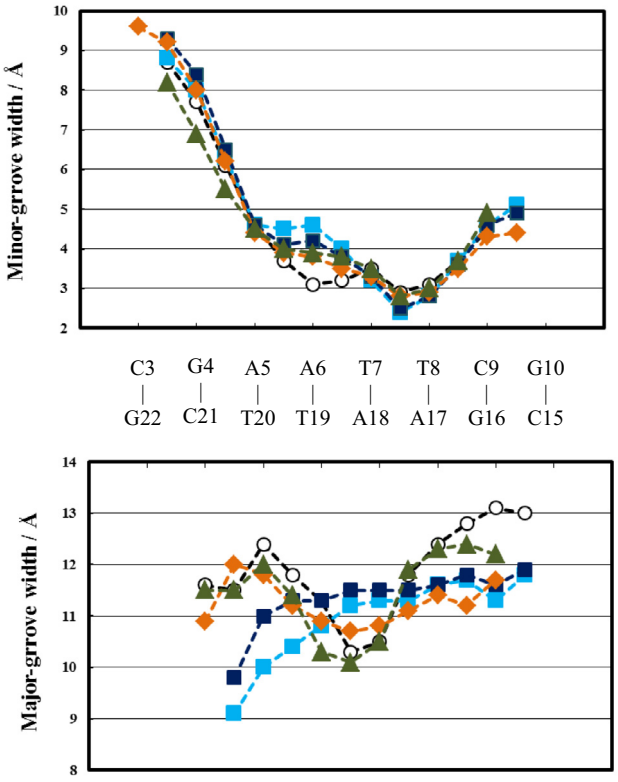

Fig. 6. Variation in minor-groove and major groove widths in PPC–DDD structures. ○: uncomplexed DDD, ■: TriplatinNC, ■: TriplatinNC/spm, ♦: TriplatinNC-A, ▲: DiplatinNC–spm. See Fig. 2 and Table 1 for abbreviations. TriplatinNC/spm is TriplatinNC–DDD crystallization in presence of spermine.

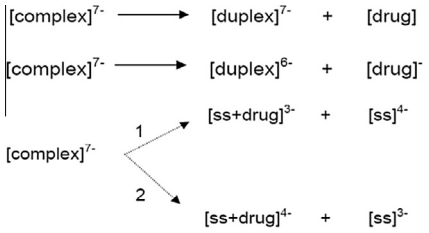

Scheme 2. Limiting gas-phase dissociation pathways for drug (ligand)–DNA complexes.

multiple phosphate clamp motifs observed from crystallography will presumably contribute to the overall gas phase stability. The energy required to separate the PPC–DNA adducts is significantly more than needed for the minor groove binding Hoechst Dye. The trend shows increasing stability in the gas phase with increasing charge and hydrogen bonding character. The mass spectral data clearly show that the dissociation pathway involves strand separation with no loss of PPC–DNA interaction, Fig. 9. These results complement those previously published for ssDNA where the binding sites could be determined by backbone cleavage of the PPC–ssDNA adduct – again no loss of PPC from the ssDNA backbone was observed [6].

4. Solution studies and binding affinities

The solid-state and gas-phase studies can now be compared to previous data obtained from solution studies [4,30,31]. The binding affinity (K_{app}) of TriplatinNC on CTDNA is significantly greater than for the minor groove binders Hoechst Dye and Netropsin and also significantly higher than the 6+ compounds **I** and **II** of Fig. 2 [30,31], Table 3. There is some sequence specificity in the binding and a combination of assays allowed delineation of groove spanning and backbone tracking [30]. Specifically, minor groove spanning was considered to be associated with A–T rich sequences while backbone tracking was more associated with G–C sequences [30]. 2D ^{1}H NMR and {^{1}H, ^{15}N} HSQCNMR studies on the TriplatinNC–DDD adduct firstly confirmed the presence of the phosphate clamp in solution and secondly confirmed the preference of groove spanning on A–T sequences [32]. These results, now taken together with the crystallography, suggest that minor groove spanning is mostly responsible for DNA bending. Anchoring the groove spanning by two phosphate clamps (one on each strand) may be an especially effective way to induce conformational changes. Comparing directly the two 6+ compounds, the trinuclear TriplatinNC-A has significantly higher affinity for poly(dA–dT)$_2$ than the spermine derivative, Table 3. These results may be consistent with the preference of the groove spanning mode on poly(dA–dT)$_2$. The spermidine compound {[{Pt(NH$_3$)$_3$}$_2$μ-(H$_2$N(CH$_2$)$_3$NH(CH$_2$)$_4$NH$_2$)]$^{5+}$ also shows similar K_{app} to the spermine analog but some very slight preference for poly(dA–dT)$_2$ [31]. The results suggest that whereas the overall binding affinity for random-sequence CTDNA may be simply related to total charge, there is some limited but high-affinity minor groove binding sites for the trinuclear species. The "classical" minor groove binders such as Netropsin and Hoechst 32258 by definition show distinct binding preferences for A–T tracts. The presence of potentially preferential A–T interactions for non-covalent polynuclear platinum complexes is indicated by protection of the minor groove toward alkylation, [33] and in all examples of PPC–DNA sequences, excepting a GC-rich sequence, studied by NMR Spectroscopy, see Table 2. In a DNAase protection assay differential cleavage plots for II are located on mostly A/T-rich sequences and A-tract regions [31]. In the latter case, little or no differential cleavage is seen for the spermine compound. Overall, the ability to engage in groove spanning correlates with preference for A–T sequences.

4.1. Nucleic acid condensation effects

UV–Vis spectroscopy, total intensity light scattering, gel retardation effects and atomic force microscopy confirm that the PPCs of Fig. 2 are all very effective in condensing nucleic acids, with TriplatinNC being the most effective [31,34]. The efficacy of various condensing agents in inducing DNA or RNA condensation can be quantified by determining the EC$_{50}$ value, the concentration of a condensing agent at the midpoint of the condensation. For CTDNA, the EC$_{50}$ value of TriplatinNC (0.15 ± 0.1 μM) is ~27-fold lower than that of spermine obtained under the same conditions, Table 3. On the other hand, the difference between **I** and **II** possessing the same charge 6+ indicates that not only overall charge but also structural properties play an important role in the condensing activity of these compounds. It has been shown that the efficiency of the condensing agent is greatly influenced by the distance between the charges in multivalent cations and is the best if there is geometrical fit between DNA phosphates and the multication charges [35]. Calf Thymus DNA can be compacted by either monomolecular condensation with distinguishable morphologies or multimolecular aggregation with irregular morphology. tRNA molecules on the other hand, are typically too short in length (60–95 nucleotides) to be individually condensed and are compacted only by multimolecular aggregation. Both trinuclear compounds are very effective in tRNA aggregation with EC$_{50}$ values of approximately 0.25 μM, slightly higher than that obtained for the condensation of CT DNA [34]. Spermine itself did not induce tRNA aggregation even at 50 μM concentration. Reflecting the high

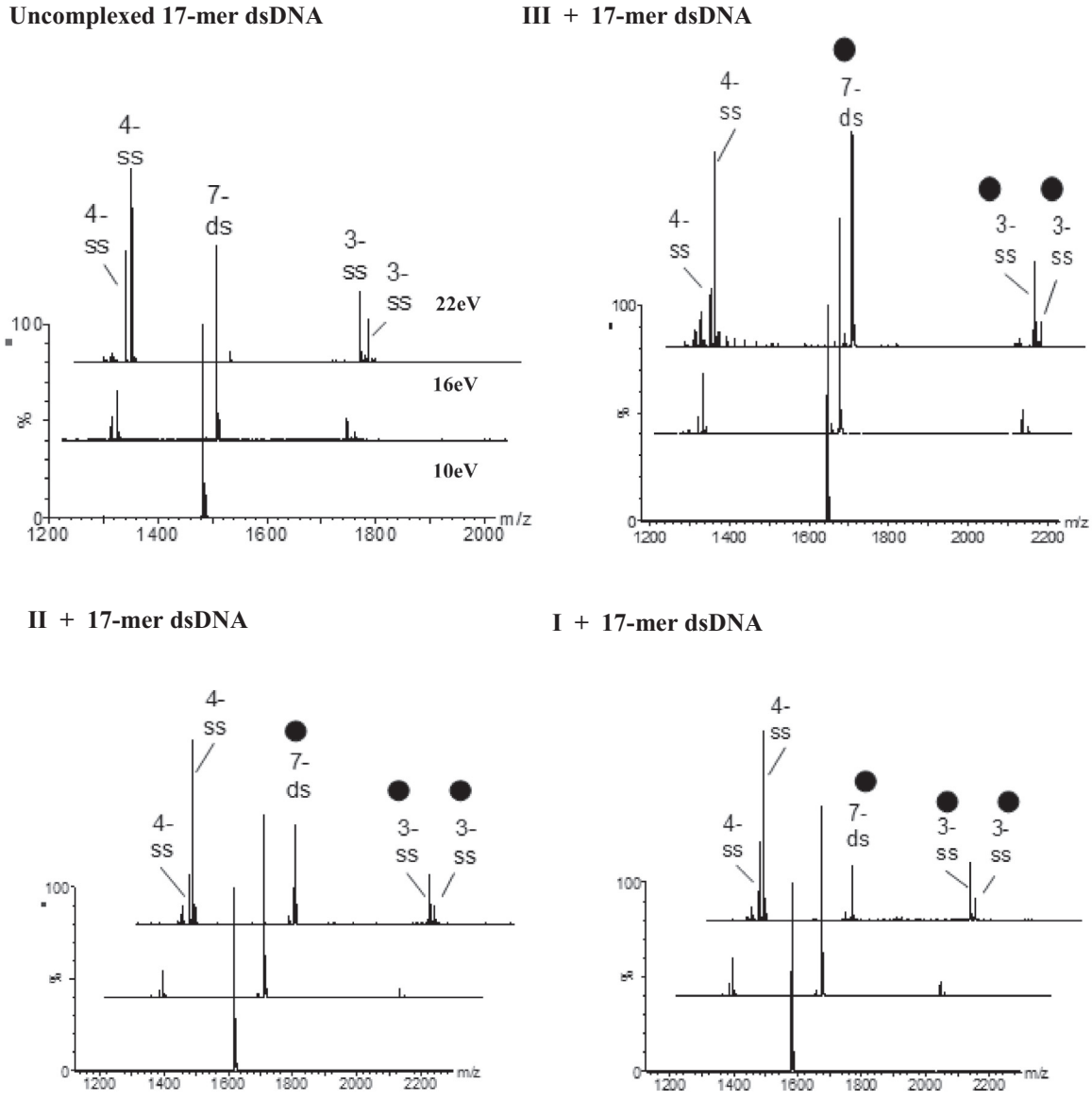

Fig. 7. Collision induced dissociation MS of the 7− charge state of 1:1 PPC-17-mer dsDNA ({5′-TAGCGCTTTTTCCGTA-3′}–{5′-TACGCGAAAAAGCGCTA-3′} adducts at increasing collisional energy of 10, 16 and 22 eV for all spectra. ● refers to the strand containing the PPC. See Supplementary information for experimental details. See Fig. 2 for full structures of **I**, **II** and **III**.

Table 2
NMR studies of substitution-inert PPC–DNA complexes.

DNA	Complex	Notes	Refs.
$d(GGTAATTACC)_2$	**II**	Similar to Hoechst dye Minor-groove contacts	[33]
d(5′-ATACAT**GG**TACATA)–d(3′ TAT**G**TACCAT**G**TAT)	**II**	Pre-association in minor groove. Affects competitive formation of inter and intra-strand crosslinks	[12]
d(5′-CGTTTTTTTTTCG)–d(3′-GCAAAAAAAAGC)	**III**	AT-rich sequence Minor-groove contacts	[30]
d(5′-AACGCGCGCGAA)–d(3′-TTGCGCGCGCTT)	**III**	GC-rich sequence Backbone tracking	[30]
$d(CGCGAATTCGCG))_2$	**III**	Dickerson–Drew Dodecamer Observation of PC in solution	[32]

affinity of phosphate clamp-oligonucleotide binding, samples containing plasmid pSP73 DNA or tRNA condensed by TriplatinNC are resistant to reversal even at high concentrations of NaCl [34]. A combination of analysis of binding affinity and conformational changes for sequence-specific oligonucleotides by ITC, dialysis, ICP-MS, CD and 2D-^{1}H NMR experiments again indicated that two limiting modes of phosphate clamp binding can be distinguished through their conformational changes and strongly sug-

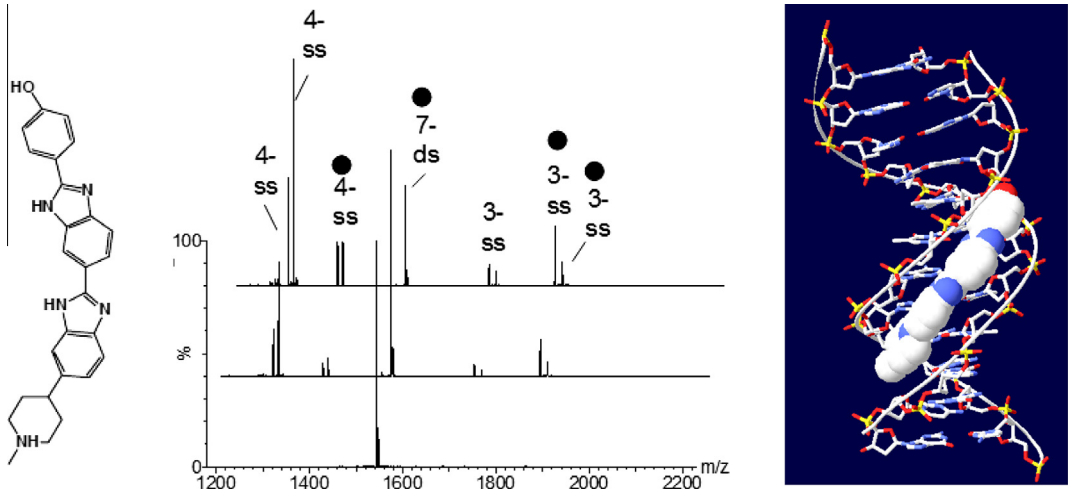

Fig. 8. Structure of Hoechst Dye 33258 (HD). CID MS at increasing voltage (10, 16, 22 eV) showing separation into ssDNA with HD on both strands (● refers to strand containing HD). Crystal structure of HD-duplex DNA PDB 264d [39].

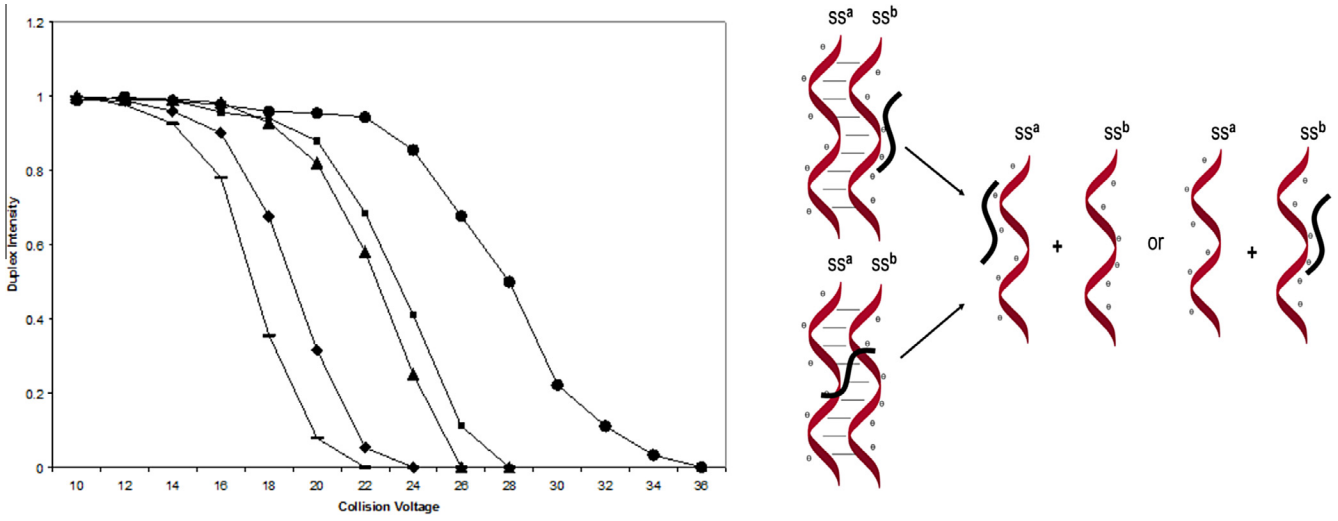

Fig. 9. Left: Duplex dissociation curve illustrating the necessary increase in applied collisional energy to achieve strand separation. – free DNA {5′-TAGCGCTTTTTCCGTA-3′}–{5′-TACGCGAAAAAGCGCTA-3′}, ◆ HD-DNA, ▲ **I**-DNA, ■ **II**-DNA, ● **III**-DNA. Right: scheme for dissociation of PPC-dsDNA in the gas phase. For full structures see Fig. 2.

Table 3
Summary of binding affinity (K_{app}) and nucleic acid condensation efficiencies (EC_{50}) for substitution-inert PPCs.

Compound	K_{app} ($\times 10^6$ M^{-1})			EC_{50} (μM)		Refs.
	CTDNA	Poly(dA–dT)$_2$	Poly(dG–dC)$_2$	CTDNA	tRNA	
Spermine	–	–	–	4.1(±0.5)	>50	[31,34]
I	34	33	33	0.25(±0.02)		[31,34]
II	36	50	39	0.20(±0.01)	0.27(±0.01)	[31]
III	56.5	–	–	0.15(±0.01)	0.24(±0.01)	[30,34]

gest that DNA condensation is also driven by minor-groove spanning [30].

5. Summary

This review complements a recent one on the chemical and biological properties of substitution-inert polynuclear platinum compounds. In all cases binding affinities are higher and conformational changes more pronounced in comparison to both free polyamines and the minor groove binder Hoechst Dye 33258. By using a spermine-linked dinuclear compound, the effects of a polyamine linker compared to the central {Pt(tetraam(m)ine} unit of trinuclear compounds can be directly compared. In the solid-state case the apparently optimal spacer between Pt coordination spheres of a hexanediamine linker is replaced with the weaker H-bonding of the polyamine unit and conformational changes are not so pronounced. The ability to engage in groove spanning requires preferably a phosphate clamp on both strands. Thus, while the total charge of the dinuclear spermine-linked compound produces global binding affinities similar to the trinuclear

TriplatinNC-A with the same 6+ charge, the differences in A–T affinity and consequent nucleic acid condensation efficiency is a reflection of the presence of the phosphate clamp – a discrete combination of the PPC structure. Thus, the overall results to date do confirm the assignation of the phosphate clamp in PPCs as a discrete third mode of ligand–DNA binding with unique properties not shared by either the structurally different intercalators or the more closely related simple charged polyamines or minor-groove binders.

Finally, while this review has not emphasized cellular effects and cytotoxicity of PPCs it is noteworthy that the substitution-inert compounds are resistant to degradation by sulfur nucleophiles, thus enhancing the pharmacokinetic stability compared to the covalently binding drugs [36,37]. The 8+ compound TriplatinNC shows *in vivo* antitumor activity, a remarkable progression from the original neutral *cis*-$[PtCl_2(NH_3)_2]$. This property added to the nucleolar targeting by these compounds, [37,38], ensure that the substitution-inert series be considered as a discrete class of antitumor agents in their own right with considerable versatility in design.

Acknowledgements

N.F. acknowledges support from NIH RO1CA78754. N.F. thanks the collaborators whose work is cited here – in alphabetical order Sue Berners-Price, Viktor Brabec, Andrew Kellett and Lawrence Povirk.

Appendix A. Supplementary material

Supplementary data associated with this article can be found, in the online version, at http://dx.doi.org/10.1016/j.ica.2016.04.052.

References

[1] Y. Qu, N.P. Farrell, Inorg. Chim. Acta 245 (1996) 265.
[2] P.J. Farmer, J.R. Cave, T.M. Fletcher Jr., J.A. Rhubottom, J.A. Walmsley, Inorg. Chim. Acta 30 (1991) 3414.
[3] N. Carte, F. Legendre, E. Leize, N. Potier, F. Reeder, J.-C. Chottard, A. Van Dorsselaer, Anal. Biochem. 284 (2000) 77.
[4] N.P. Farrell, Chem. Soc. Rev. 44 (2015) 8773.
[5] N.P. Farrell, Drugs Future 37 (2012) 795.
[6] J.B. Mangrum, N.P. Farrell, J. Chem. Soc., Chem Commun. 46 (2010) 6640.
[7] S.J. Berners-Price, L. Ronconi, P.J. Sadler, Prog. NMR Spectrosc. 49 (2006) 65.
[8] A. Hegmans, S.J. Berners-Price, M.S. Davies, D.S. Thomas, A.S. Humphreys, N.P. Farrell, J. Am. Chem. Soc. 126 (2004) 2166.
[9] M.B.G. Kloster, J.C. Hannis, D.C. Muddiman, N. Farrell, Biochemistry 38 (1999) 14731.
[10] J. Malina, N.P. Farrell, V. Brabec, Chem. Asian J. 6 (2011) 21566.
[11] R.A. Ruhayel, J.J. Moniodis, X. Yang, J. Kasparkova, V. Brabec, S.J. Berners-Price, N.P. Farrell, Chem. Eur. J. 15 (2009) 9365.
[12] J.J. Moniodis, D.S. Thomas, M.S. Davies, S.J. Berners-Price, N.P. Farrell, J. Chem. Soc., Dalton Trans. 44 (2015) 3583.
[13] H. Rauter, R. Di Domenico, E. Menta, A. Oliva, Y. Qu, N. Farrell, Inorg. Chem. 36 (1997) 3919.
[14] N. Farrell, Y. Qu, U. Bierbach, M. Valsecchi, E. Menta, in: B. Lippert (Ed.), 30 years of Cisplatin – Chemistry and Biochemistry of a Leading Anticancer Drug, Verlag, 1999, p. 479.
[15] T.D. McGregor, J. Kasparkova, K. Neplechova, O. Novakova, H. Penazova, O. Vrana, V. Brabec, N. Farrell, J. Biol. Inorg. Chem. 7 (2002) 397.
[16] P. Wu, M. Kharatishvili, Y. Qu, N. Farrell, J. Inorg. Biochem. 63 (1996) 9.
[17] T.D. McGregor, W. Bousfield, Y. Qu, N. Farrell, J. Inorg. Biochem. 91 (2002) 212.
[18] S. Komeda, T. Moulaei, K.K. Woods, M. Chikuma, N.P. Farrell, L.D. Williams, J. Am. Chem. Soc. 128 (2006) 16092.
[19] S. Komeda, T. Moulaei, M. Chikuma, A. Odani, R. Kipping, N.P. Farrell, L.D. Williams, Nucleic Acids Res. 39 (2011) 325.
[20] Y. Qu, A. Harris, A. Hegmans, A. Petz, H. Penazova, N. Farrell, J. Inorg. Biochem. 98 (2004) 1591.
[21] N. Farrell, Metal Ions Biol. Syst. 41 (2004) 252.
[22] F. Rosu, S. Pirotte, E.D. Pauw, V. Gabelica, Int. J. Mass Spectrom. 253 (2006) 156.
[23] J.L. Beck, M.L. Colgrave, S.F. Ralph, M.M. Sheil, Mass Spectrom. Rev. 20 (2001) 61.
[24] A.S. Woods, J. Proteome Res. 3 (2004) 478.
[25] S. Alves, A. Woods, A. Delvolv, J.C. Tabet, Int. J. Mass Spectrom. 278 (2008) 122.
[26] S.N. Jackson, H.Y. Wang, A.S. Woods, J. Proteome Res. 4 (2005) 2360.
[27] A.S. Woods, S.C. Moyer, S.N. Jackson, J. Proteome Res. 7 (2008) 3423.
[28] K. Schug, W. Lindner, Int. J. Mass Spectrom. 241 (2005) 11.
[29] K. Ohara, M. Smietana, J.-J. Vasseur, J. Am. Soc. Mass Spectrom. 17 (2006) 28.
[30] A. Prisecaru, Z. Molphy, R.G. Kipping, E.J. Peterson, Y. Qu, A. Kellett, N.P. Farrell, Nucleic Acids Res. 42 (2014) 13474.
[31] J. Malina, N.P. Farrell, V. Brabec, Inorg. Chem. 53 (2014) 1662.
[32] Y. Qu, R.G. Kipping, N.P. Farrell, Dalton Trans. 44 (2015) 3563.
[33] Y. Qu, J.J. Moniodis, A.L. Harris, X. Yang, A. Hegmans, L.F. Povirk, S.J. Berners-Price, N.P. Farrell, in: P.M. Woster (Ed.), Polyamine Drug Discovery, Royal Society of Chemistry, Cambridge, 2012, p. 1914.
[34] J. Malina, N.P. Farrell, V. Brabec, Angew. Chem., Int. Ed. 53 (2014) 12812.
[35] A.A. Zinchenko, V.G. Sergeyev, K. Yamabe, S. Murata, K. Yoshikawa, ChemBioChem 5 (2004) 360.
[36] B.T. Benedetti, E.J. Peterson, P. Kabolizadeh, A. Martínez, R. Kipping, N.P. Farrell, Mol. Pharmacol. 8 (2011) 940.
[37] E.J. Peterson, V.R. Menon, L. Gatti, R.G. Kipping, P. Perego, L.F. Povirk, N.P. Farrell, Mol. Pharm. 12 (2015) 287.
[38] L.E. Wedlock, M.R. Kilburn, R. Liu, J.A. Shaw, S.J. Berners-Price, N.P. Farrell, J. Chem. Soc., Chem. Commun. 49 (2013) 6944.
[39] C. Vega, I. Garcia Saez, J. Aymami, R. Eritja, G.A. van der Marel, J.H. van Boom, A. Rich, M. Coll Eur, J. Biochem. 222 (1974) 721.